The 21st Conference of Mechanical Engineering Network of Thailand
17-19 October 2007, Chonburi, Thailand

Experimental study of impact-generated high-speed liquid jet

Anirut Matthujak [1]*, Kulachate Pianthong [1], Mingyu Sun [2] and Kazuyoshi Takayama [2]

[1] Department of Mechanical Engineering, Faculty of Engineering, Ubon Ratchathani University,
Ubon Ratchathani, 34190, Thailand,
Tel: +66-45-353380, Fax: +66-45-353333, *Email: Anirut.Mat@gmail.com, A.Matthujak@ubu.ac.th
[2] Interdisciplinary Shock Wave Research Laboratory, Institute of Fluid Science, Tohoku University,
Sendai, 980-8577, Japan,
Tel: +81-22-2175285 ext 5286

Abstract

More detailed high-speed liquid jet structures ejected into ambient air are reported in this paper. High-speed liquid jets are generated by impact acceleration method in a vertical two-stage light gas gun. In this study, double exposure holographic interferometry, which this method is versatile enough to visualize shock waves in gases, liquids and transparent solids and in reactive media, was applied to quantitatively observe the jet formation of water, diesel fuel, kerosene, and gasoline jet speed of 1.3 km/s. In the interferogram images, we can clearly observe not only more detailed jet structures but also the shocked air, core parts of the jets, jet boundaries, air/liquid vapor mixture zone, and liquids, which are indicated by interferograms fringes. Nevertheless, the high-speed video camera was used to record shadowgraph images of such jets formations and to evaluate the jet velocity and penetration distance. Dynamic characters of liquid jets such as jet formation and attenuation and, in particular, multiple intermittent acceleration were displayed. Moreover, we examined the possibility of auto-ignition over high-speed liquid fuel jets, and then found that no auto-ignition took place on all liquid fuel jets ejected into ambient air.

Keywords: High-speed liquid jet, Impact acceleration method, Double exposure holographic interferometry, Shock wave

1. Introduction

The generation of high-speed liquid jets is one of the fundamental research topics of high-speed gas dynamics. High-speed liquid jets were produced traditionally by discharging liquid through a nozzle or an orifice connected to pressurized liquid chambers at static pressure of sub GPa but the storage has a technical limitation.

To overcome the technical limitation of confining liquids in static high-pressure vessels, Bowden and Brunton [1, 2] generated, for the first time, extreme high-pressures by the impingement of high-speed projectiles against a liquid filled container and recorded, by using a high-speed photography, a water jet of 1200 m/s. Their main concern was to apply this technique to study the erosion of jet impinged solid surfaces. Since then, extensive studied have been carried out by many researchers [3, 4, 5]. In 1967, O'Keefe et al. [6], using the same principle as Bowden and Brunton [1, 2] successfully generated water jet speeds up to 4.58 km/s.

Many researchers also produced high-speed jets by refining impact acceleration method to match with their own research purposes [7, 8, 9]. In 1976, Edney [10] produced a 3.5 km/s jet at an impact pressure up to 1.8 GPa and found that nozzle geometries significantly influenced to the maximum water jet speed. In particular, nozzle shapes of exponential and hyperbolic profiles were used.

In 1977, Field and Lesser [11] investigated experimentally and analytically supersonic liquid jet flows and predicted self-combustion of oil jets at high supersonic jet speeds, because partial auto-ignition took place in their oil fuel jets injected even in ambient air.

In 1992, Shi [12-15] visualized high-speed liquid jets at supersonic to hypersonic speeds, uniquely using double exposure holographic interferometry and studied liquid-jet impact on liquid and solid surface [16, 17], shock waves generation over high-speed jets [18, 19], and auto-ignition feasibility of supersonic diesel fuel jet [20]. He described the jet characteristics up to 3 km/s and claimed that the sign of auto-ignition at a 2 km/s diesel jet in atmospheric air. The temperature behind the shock wave at stagnation regions of a diesel fuel jet is high enough to induce the auto-ignition.

Subsequently, Pianthong [21, 22] studied the generation of supersonic liquid jets and jet-induced shock waves by using shadowgraph method, clarified the effect of nozzle geometries on jet speeds, jet shapes and shock wave angles [23], and, in particular, analyzed, for the first time, the multiple pulsed supersonic diesel fuel jet formation [24, 25] based on a simple one-dimension

model [26]. He obtained a negative result regarding the induction of auto-ignition over a 2 km/s diesel fuel jet in atmospheric air.

As the previous studies, visualization is one of the most suitable methods in studying the high-speed liquid jet. Most of previous visualization technique used in the high-speed liquid jet study is shadowgraph method. Moreover, most of previous studies of high-speed jets have handled with only water and diesel fuel at supersonic to hypersonic speeds [6-26]. For the jet speed exceeding 2 km/s, it is likely hard to use benefits of high-speed jets for practical applications. If one wishes to expand the basic high-speed jet formation to practical uses in the near future, at first we should clearly understand the jet characteristics in the speed range of slower than 1.4 km/s. In this paper, the high-speed jet formation based on the impact acceleration method is described by using double exposure holographic interferometry. The speed of jet tips, their dynamic characteristics such as their formation and attenuation; and their multiple intermittent accelerations are clarifie by .a high-speed video camera with shadowgraph arrangement. We tested with water, diesel fuel, kerosene, and gasoline jet at jet speeds of 1.3 km/s. We eventually concluded a negative result of auto-ignition on all the liquid fuel jets.

2. Experimental facility

In this study, high-speed liquid jet is generated by a technique known as the projectile impact driven method [23]. The liquid fuel retained in the nozzle cavity is impacted by a high velocity projectile. The liquid fuel, absorbing the momentum and energy transmitted from the projectile, are injected from the nozzle orifice. The high velocity projectile needed in this technique has been launched by the vertical two stage light gas gun (VTSLGG), shown in Fig. 1. The VTSLGG consists of a 50 mm diameter and 1.50 m long high pressure reservoir, and a 50 mm diameter pump tube (2 m in length).The launch tube has a diameter of 15 mm and length of 1 m The pressure relief section has a length of 53 cm, which is designed to diminish the blast wave in front of the projectile. The pressure relief section has 3 columns of the relief holes, each hole having a diameter of 8 mm. The total height of the VTSLSS is around 6 m. The projectile velocity of around 323.5 m/s was used to generate all supersonic liquid jet in this experiment. The component detail and the operation procedure of the VTSLGG have been described [25].

Fig. 2 shows the piston, the projectile and the nozzle used in this paper. The projectile, 20 mm long and 15 mm in diameter, is made of polycarbonate and weights 4.2 g. The piston used in the pump tube is made of high density polyethylene (HDPE), has a diameter of 50 mm and length of 75 mm (weight of 130 g). The nozzle that is connected to launch tube is made of mid-steel, and its dimension is shown in Fig. 2c.

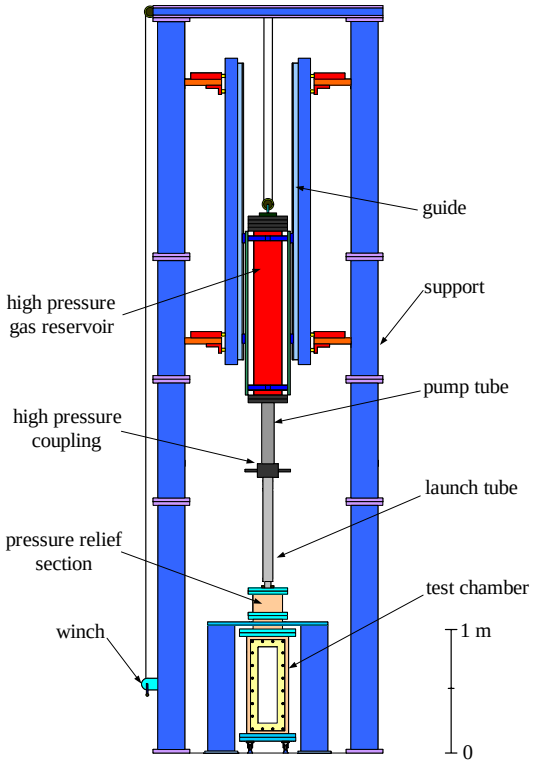

Figure 1. Vertical two-stage light gas gun (VTSLGG)

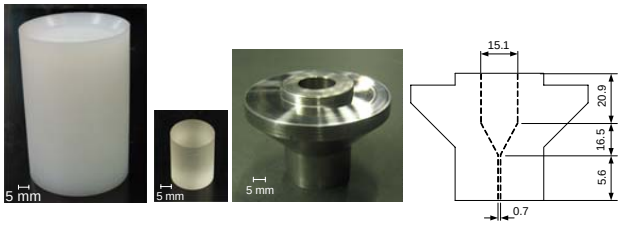

Figure 2. (a) Piston (b) projectile (c) nozzle geometry

3. Visualization method

3.1 Shadowgraph for high-speed video recording

We used a high-speed video camera and shadowgraph optical arrangement as shown in Fig. 3. The dynamic jet formation and unsteady projectile motions are quantitatively measured by sequential observations. A flash lamp is used as light source. The source light is collimated passing through a circular slit and a concave lens. The flash light interval is 2 ms and rise time of 250 μs. The laboratory space is so limited that we combined plane mirrors of diameter 150 mm, 200 mm, and 300 mm and a rectangular plane mirror of 240 mm x 600 mm. Two paraboloidal schlieren mirrors of diameter 500 mm were used for collimating source light beam passing the test section area. A convex lens was used to focus the object image on the high-speed video camera screen. The high-speed video camera is a Shimadzu HPV-1 at frame rate of up to 1,000,000 f/s, exposure time of 1/4 of inter-frame time, and the total number of images of 104. The test section has 20 mm thick acrylic windows and its view field is 150 mm x 650 mm.

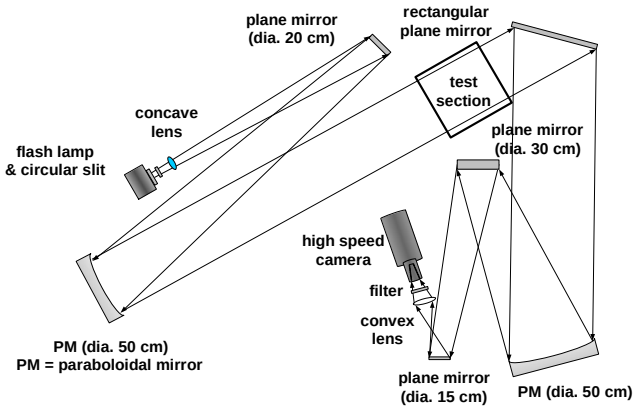

Figure 3. Shadowgraph optical setup for high-speed video recording

3.2 Double exposure holographic interferometry

Since 1975, Takayama [27] started to use double exposure holographic interferometry to shock wave research convincing that this method was versatile enough to visualize shock waves in gases, liquids and transparent solids and in reactive media. This technique, unlike other flow visualization methods which detect the changes of refractive index associated with shock induced density variations, can detect the phase change in media modulated by density variations which occurred during double exposures. Therefore, this visualization method is not decisively influenced by the quality of elements in optical alignments, and is free from in-homogeneity and non-uniformity of media, which are mostly caused by density variations due to natural convection. This optical arrangement is based on that of direct shadowgraph and is readily convertible to the shadowgraph arrangement.

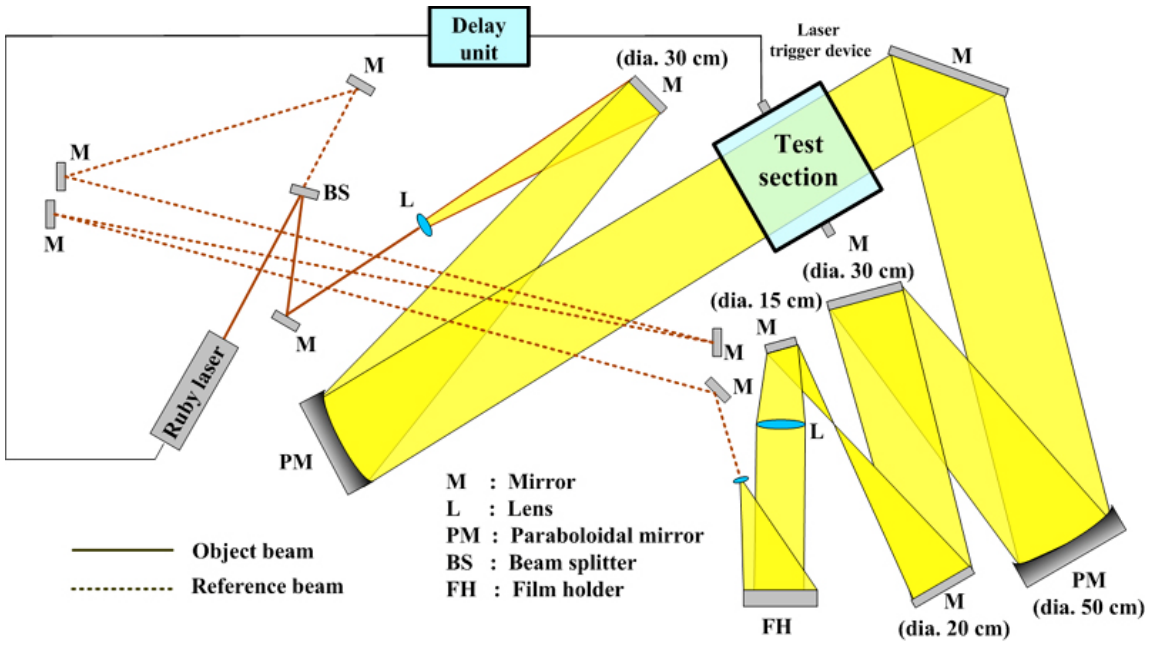

Figure 4. Double exposure holographic interferometric arrangement

Figure 4 shows a double exposure holographic interferometric arrangement. Light source is a holographic ruby laser (Innolus HLS/R20, wavelength of 694 nm, 15 ns pulse duration and pulse energy 1.0 J/pulse). We used a 6:4 beam splitter and the source laser beam was split 60% into an object beam (OB) and 40% into a reference beam (RB). Using plane mirrors of diameter 150 mm, 200 mm, and 300 mm mirrors, a rectangular plane mirror of 240 mm x 600 mm and other mirrors, OB path and RB path were formed in nearly identical path lengths. Two 500 mm diameter paraboloidal schlieren mirrors 5 m in focal length were used for collimating OB passing the test section. A convex lens was placed in the film side to focus the object image on a 100 mm x 125 mm holographic sheet film tightly fixed on a film holder. RB was collimated with a plano-convex lens and then illuminated on the holofilm. Film was a 100 mm by 125 mm Agfa-Gevaert sheet holofilm, 2RDQ1.

First and second exposures were successively performed. Sometimes the first exposure was performed manually prior to the event and the second exposure was synchronized with the event. If OB and RB paths were totally unchanged during the two exposures, density variations proportional to refractive index variations are displayed in the form of distributed interference fringes. Such interference images were called infinite fringe interferograms. These fringes so far recorded on holograms contain information of phase difference, which appeared during the two exposures and was extracted only through a process of reconstruction.

The present holographic system is named as image

hologram and unreconstructed images on a holofilm are equivalent to shadowgraph images. Illuminating holograms obliquely by a collimated laser beam by using the same optical setup as RB, we have virtual OB images with distributed fringes. Then we recorded OB images by a CCD camera or by using an image focus lens directly on a sheet film. This process is named reconstruction as shown in Fig. 5. A continuous Argon-ion laser beam of wavelength 514.5 nm was used for reconstruction. We used a 150 mm diameter plano-convex lens to reconstruct virtual OB images on 100 mm x 125 mm Fuji NoePan SS sheet film. The exposure of reconstruction took about one second.

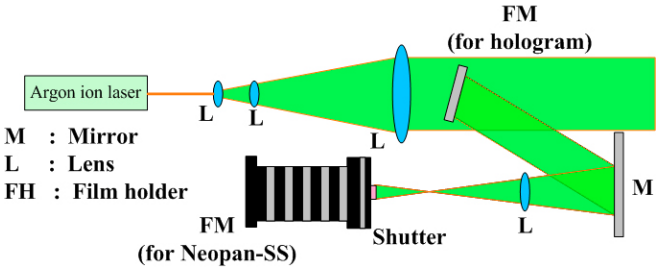

Figure 5. Reconstruction arrangement

4. Jet formation

Using a high-speed video camera, Shimadzu HPV-1 could record shadowgraph images at total number of frames of 104 at frame rate of up to 1,000,000 f/s and exposure time of 250 ns. Such a sequential recording is very useful to observe the jet formation.

In Fig. 6, only selective 8 images are presented where the image width is always 150 mm. In Fig. 6a, jet formations of water at V_p = 317 m/s, in Fig. 6b diesel fuel at V_p = 295 m/s, in Fig. 6c kerosene at V_p = 305 m/s, and in Fig. 6d gasoline at V_p = 295 m/s are compared and the individual liquid properties are listed in Table 1, where V_p denotes the projectile speed and all the jets were discharged into atmospheric air.

The water jet shows the slimmest width among all others and looks more elongated to be over 350 mm at 320 μs. Its averaged speed at 320 μs is 1.094 km/s and Ms = 3.21 in room temperature air. The jet motion is supersonic so that oblique shock waves are created over its top part and also the jet's nodes. At the earlier stage, the inclination angle of the first oblique shock wave is about 18^o which corresponds to the oblique shock Mach number of 3.24, whereas the observable shock speed from high-speed images is 1.345 km/s and Ms = 3.94.

The jet speed estimated from the shock inclination angle differs from that obtained from the video images. This is attributable to the fact that the relationship between the oblique shock angle and a supersonic body is valid to a supersonic solid body but in this case the jet boundary consists of distributed liquid droplets/air mixture and irregularly shaped water surface. The sound speed defined around such a jet boundary is no longer the same as that of air and slightly smaller than that in air.

In addition to this fact, the liquid jet's frontal stagnation area has a dispersed structure and a kind of ablation takes place. Not only fragmentation from bulk liquid to droplets but also vaporization on the liquid surface simultaneously takes place. As a result of it, the corresponding inclination angle of shock wave and the shock stand off distance over the liquid jet not necessarily coincides with those over a solid body moving at the identical supersonic speed. The discrepancy also exists between the estimated jet speed from shock inclination angle and that from the video images.

The jet shape in water appears to be less disturbed than other liquid jets. Jets are accelerated intermittently and then, at least, three nodes are observable in the entire jet length. The water jet speed is the fastest among other liquid jets but its attenuation occurs very slightly with the elapse of time.

Figure 6b shows diesel fuel jet formation. The nodes observable over the entire diesel fuel jet look bulkier than those in water jet. This trend is commonly seen in kerosene and gasoline, which is attributable to smaller values of surface tension and heat capacity. The jet surface can expand relatively easier than in less volatile. In liquids having larger surface tension liquid the jet will not expand even at intermittent pressure loadings and resulting sizes of node will be smaller.

Table 1. Properties of liquid used in the experiment

Liquid type	Density at 293 K (Kg/m^3)	Kinematic viscosity at 293 K (mm^2/s)	Surface tension at 293 K (Kg/s^2)	Heat capacity at 313 K (J/gK)	Latent heat (at boiling temperature) (kJ/kg)	Sound speed at 293 K (m/s)
Water	998	1.007	0.0717	4.187	2260 (at 373 K)	1483
Diesel fuel	840	1.8 – 4.0	0.0244	1.97	267.49 (at 443 K)	1350
Kerosene	810	1.5 – 2.5	0.0235	2.02	314.01 (at 390.8 K)	1324
Gasoline	750	0.5	0.02	2.1	318.66 (at 363 K)	-

Acoustic impedances of diesel fuel, kerosene, and gasoline are smaller than that of water. Hence, pressures generated at projectile impingements are less than that in water even at small impact speed. This explains the reason why the faster jet speed is generated in water. The diesel fuel jet appears to be elongated even more than 350 mm at 376 μs and its speed is slower than the water jet.

Figure 6c shows kerosene jet formation. Three steps of impulsive accelerations are clearly observed at 128 μs. The general trend of the kerosene jet formation is similar to the diesel jet formation. The jet is attenuated as its leading edge is not elongated as quickly as seen in the last three frames from 320 to 440 μs. Detached shock waves are clearly visible on the second and the third frames.

Figure 6d shows gasoline jet formation. The projectile speed is not as fast as other cases, but to the general trend is not very different from diesel fuel and kerosene jets up to 480 μs. Gasoline is a very volatile liquid and hence the largely disturbed jet boundary would promote further vaporization. The jet boundary on images after 480 μs looks blurred. Shock wave is attached at the jet's leading edge but after 480 μs it becomes a detached shock wave due to the shock attenuation.

As seen in Fig. 6, jet tips and frontal parts of nodes have dispersed structures and their boundaries are blurred. Hence, distinct shock fronts are not observable but trains of compression waves are formed, which at later time coalesce into oblique shock fronts. At the earlier stage of their formations, their boundary edge looks not necessarily clear but obscure.

In order to optimize liquid acceleration, we need to maintain high plateau pressures for some short duration of time by optimizing nozzle shapes so as to match with liquid properties, for example, a conical nozzle as shown in Fig. 2c. Depending on the nozzle geometry and impact velocity, we will be able to adjust the generation and reflection of shock waves and hence the multiple intermittent jet accelerations (described in detail in [23]).

Figure 7 shows sequential interferograms of jet formations: in Fig. 7a, water at V_p = 350 m/s and interferograms were taken at 144 μs, 176 μs, and 248 μs; in Fig. 7b, diesel fuel at V_p = 342 m/s and interferograms were taken at 112 μs, 168 μs, and μs; in Fig. 7c kerosene at V_p = 347 m/s and interferograms were taken at 128 μs, 320 μs, and 440 μs; and in Fig. 7d, gasoline at V_p = 339 m/s and interferograms were taken at 56 μs, 160 μs, and 480 μs are compared.

The trend of jet formations in individual liquids is similar to high-speed video images in Fig. 6. However, more detailed jet structures are observable. As the interferometry is sensitive to the variations of refractive index, it varies depending on concentration of liquid vapor in the mixture. Therefore, the image contrast along the boundaries of liquid jets is distinctly different from the core parts of the jets, which indicates the difference of refractive indices among the shocked air, air/liquid vapor mixture zone, and liquids. The mixing zone in gasoline at 480 μs is the broadest whereas in water and diesel fuel the mixing zone area is smaller. Shock shapes vary corresponding to those of jet boundaries, which clearly indicates processes of intermittent accelerations.

Fig. 7a shows the effect of different liquid types on the average jet velocity. The average jet velocity of water, diesel fuel and kerosene jet are similar, but the velocity of gasoline jet is difference being the slowest. During the maximum velocity point and the emerging time of 100 μ s, the velocity of gasoline jet drops quickly as obviously seen in the figure. That effects on the penetration distance of gasoline jet being shorter than that of all jets as shown in Fig. 7b. In the figure, the penetration distance of water, diesel fuel and kerosene jet are similar, since their velocities are similar. The different characteristic of gasoline jet from all fuel jets is an interesting point that still needs more experiment to clearly describe or confirm the occurrence.

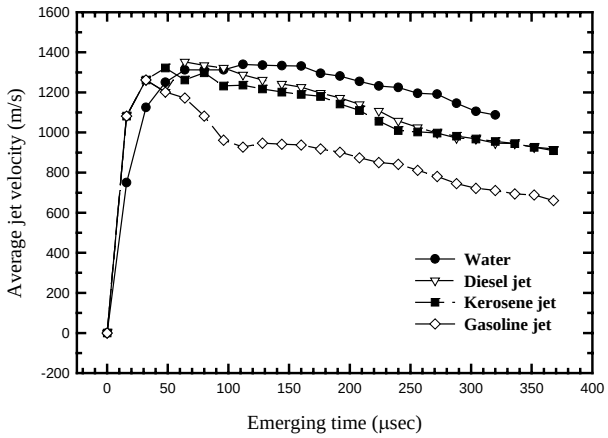

(a)

(b)

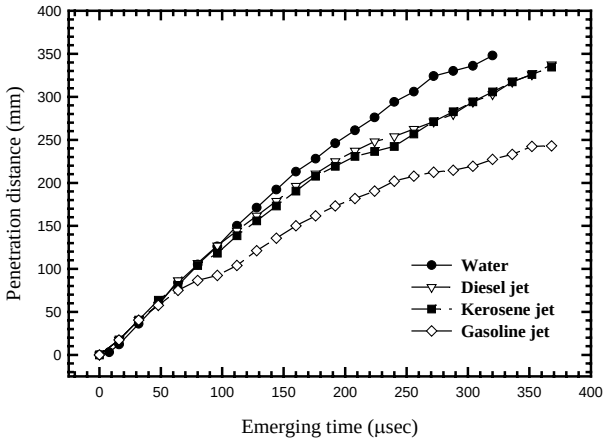

Figure 7. Effect of difference liquid fuels on (a) average jet velocity (b) jet penetration distance

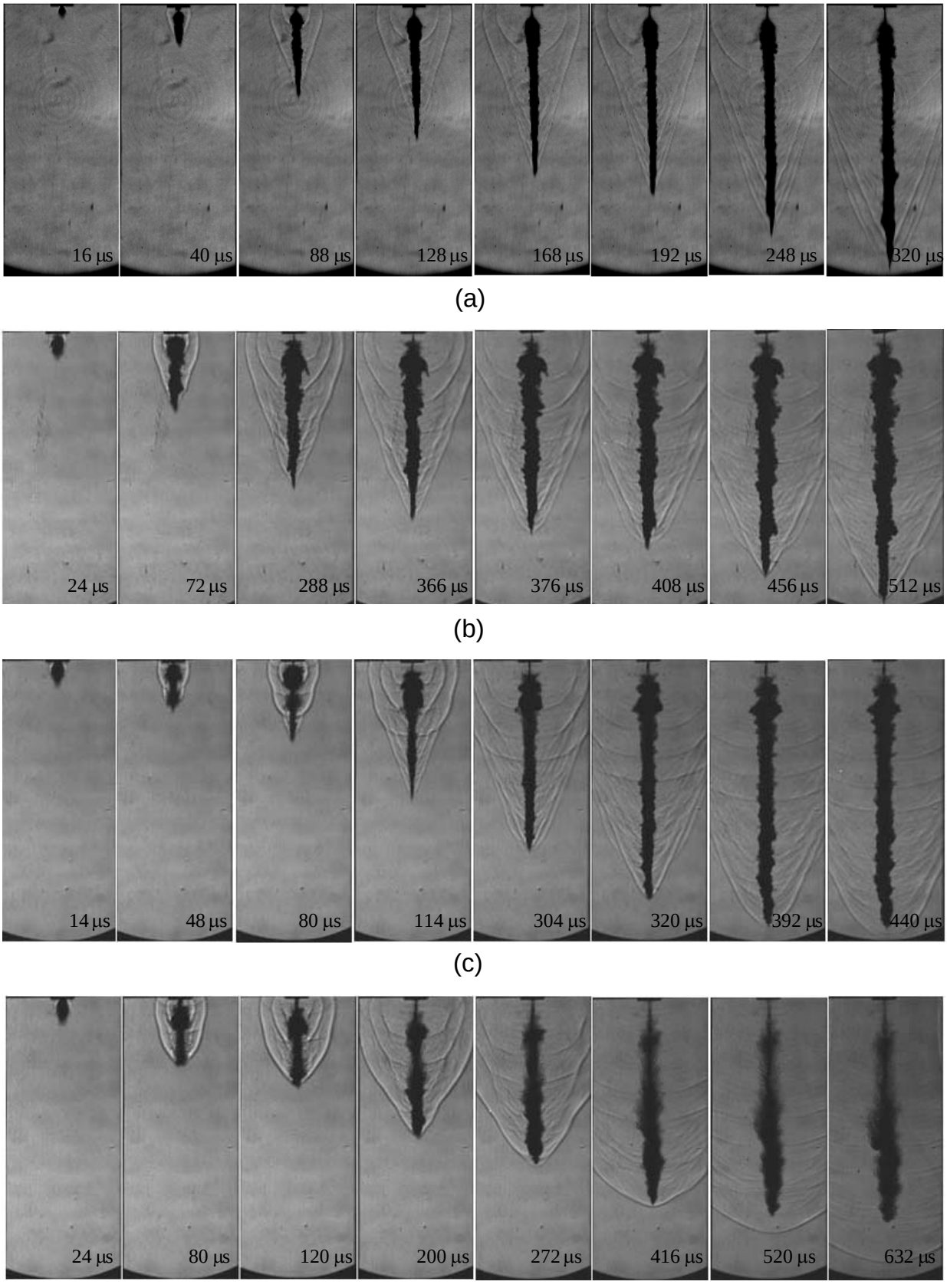

Figure 6. Jet formation (a) Water, V_p = 317 m/s; (b) Diesel fuel, V_p = 295 m/s; (c) Kerosene, V_p = 305 m/s; and (d) Gasoline, V_p = 295 m/s. Notice shock waves over jets. The width of each frame is 150 mm.

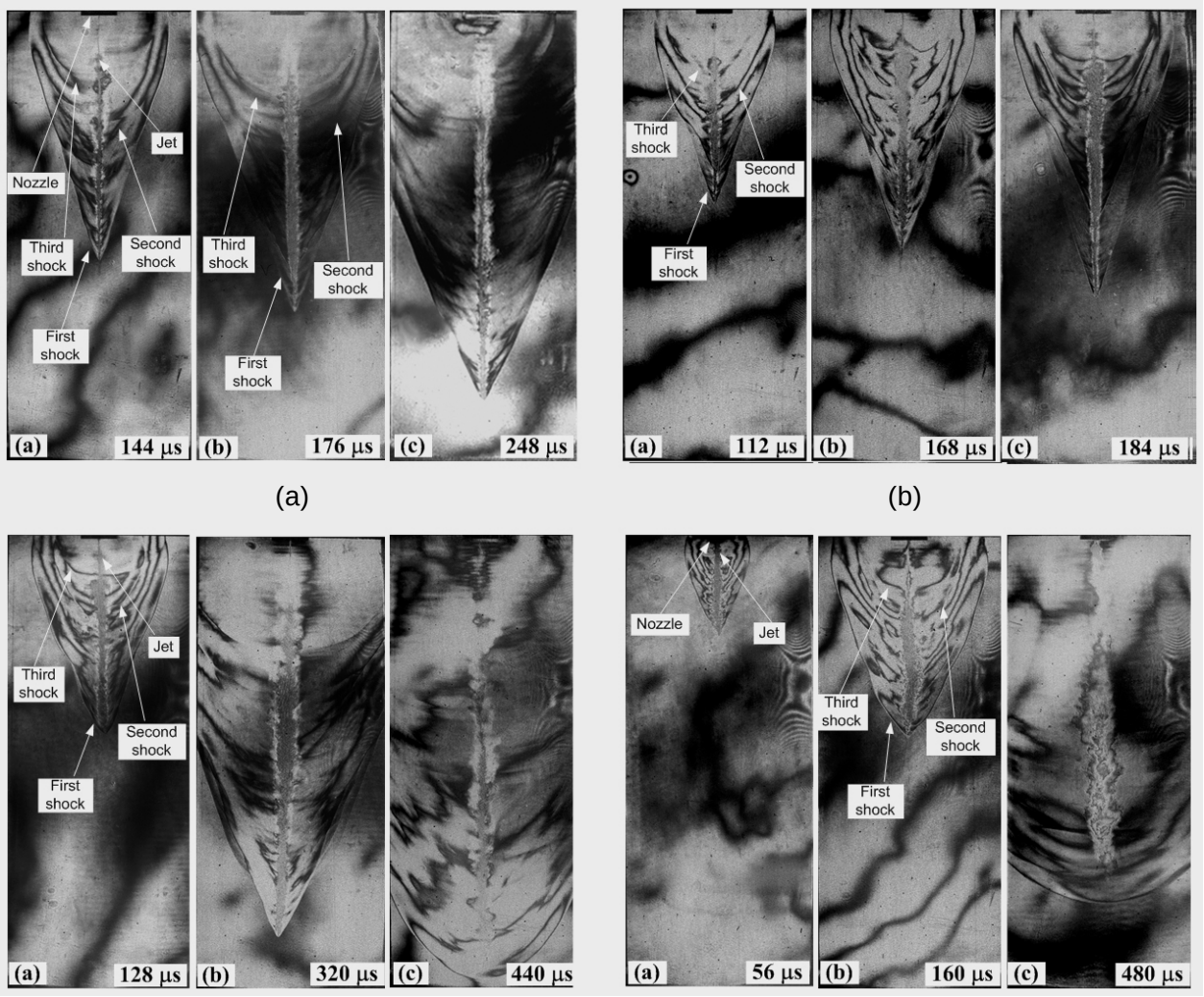

Figure 7. Holographic interferograms of (a) Water jet formation, $V_p = 359 \pm 10$ m/s; (b) Diesel fuel jet formation, $V_p = 352 \pm 5$ m/s (c) Kerosene jet formation, $V_p = 357 \pm 9$ m/s; (d) Gasoline jet formation, $V_p = 349 \pm 15$ m/s.. Notice that shock waves are generated intermittently over jets and air/liquid mixtures along the jet interface

5. Conclusions

High-speed jets of water and other liquid fuels were generated by impact acceleration method. The liquid jet formation and its characteristics were examined by using double exposure holographic interferometry and a high-speed video camera based on shadowgraph arrangement. Results obtained are summarized as following:

(1) The 0.7 mm diameter conical nozzle generated multiple intermittent jet formations.

(2) By optical flow we successfully observed the dynamics of water, diesel fuel, kerosene, and gasoline jet formations and individual jet structures at projectile impingement velocities ranging from 300 m/s. Jet characteristics vary depending on physical properties of liquids.

(3) At projectile impact velocity of about 300 m/s, the liquid jet speed was 4 to 4.5 times as high as the impact velocity.

(4) The intermittent jet formation was achieved by optimizing the nozzle geometry and impact velocity, for example, a conical container with 0.7 mm diameter nozzle designed to match with liquid properties and at the impact velocity of 300 m/s.

(5) The possibility of auto-ignition was examined for all the liquid fuel jets ejected into ambient air. Despite of the presence of favorably high temperature behind the bow shock in front of the jet tip, we convinced that auto-ignition never occurred.

Acknowledgments

We wish to acknowledge Mr. S. Haysaka of Tohoku University for his encouragement and devotion in conducting the present experiments and all staff members of the Interdisciplinary Shock Wave Research Laboratory. We also wish to express gratitude to T. Kikuchi and D. Numata who helped in setting up the optical system. The first author would like to express his acknowledgement to Royal Thai Government for financial support. This project was in part supported by the Grant-in-Aid for Science Research No. 12 CE 2003

offered by the Ministry of Education, Culture, Sport, Science and Technology, Japan.

References

[1] Bowden, F.P., and Brunton, J.H., 1958. Damage to solids by liquid impact at supersonics speeds. Nature, Vol. 181, pp. 873-875.

[2] Bowden, F.P., and Brunton, J.H., 1961. The deformation of solids by liquid impact at supersonic speeds. Proc Royal Society London, Vol. 263 (series A), pp. 433–450.

[3] Shi, H.H., and Dear, J.P., 1992. Oblique High-speed liquid-solid impact. JSME Int J Series I**,** Vol. 35, No. 3, pp. 285-295.

[4] Lesser, M., 1995. Thirty years of liquid impact research: a tutorial review. Wear, Vol. 186-187, pp. 28–34.

[5] Obara, T., Bourne, N.K., and Field, J.E., 1995. Liquid-jet impact on liquid and solid surfaces. Wear Vol. 186-187, No. 2, pp. 388-394.

[6] O'Keefe, J.D., Wrinkle, W.W., and Scully, C.N., 1967. Supersonic liquid jets. Nature, Vol. 213, pp. 23-25.

[7] Rochester, M.C., and Brunton, J.H., 1972. High speed impact of liquid jets on solid. 1st Int Symp Jet Cutting Technology, Coventry, UK, A1.1–A1.

[8] Hirano, N., and Takayama, K., 1997. Hydrodynamics of droplet impingement on surface. 21st Int Symp Shock Waves, paper no. 5839.

[9] Pater, L.L., 1984. Experiments with a cumulation pulsed jet device. 7th Int Symp Jet Cutting Technology, pp. 83–90.

[10] Edney, B.E., 1976. Experimental studies of pulsed water jets. 3rd Int Symp Jet Cutting Technology, B2.11–B2.26.

[11] Field, J.E., and Lesser, M.B., 1977. On the mechanics of high speed liquid jets. Proc Royal Soc London 357 (Series A), pp. 143-162.

[12] Shi, H.H., 1994. Study of Hypersonic Liquid Jets. Ph.D. thesis, Tohoku University, Sendai, Japan, pp. 1-186.

[13] Shi, H.H., Takayama, K., and Onodera, O., 1994. Supersonic diesel fuel injection through a single-hole nozzle in a compact gas gun (part 2). JSME Int J Series B, Vol**.** 37, No. 3, pp. 509–516.

[14] Shi, H.H., Koshiyama, K., and Itoh, M.1996. Further study of the generation technique of high-speed liquid jets and related shock wave phenomena using a helium gas gun. Japanese J Appl Physics, Vol. 35, No. 7, pp. 4147–4156

[15] Shi, H.H., and Itoh, M., 1998. Generation of high-speed liquid jet from a rectangular nozzle. Trans Japan Soc Aero and Space Sci, Vol. 41, No. 134, pp. 195–202.

[16] Shi, H.H., Field, J.E., and Pickles, C.S.J., 1994. High speed liquid impact onto wetted solid surfaces. J Fluids Eng, Vol. 116, pp. 345-348.

[17] Shi, H.H., Higashiura, K., and Itoh, M., 1999. Generation of hypervelocity liquid jets using a powder gun and impact experiment. Trans Japan Soc Aero and Space Sci, Vol. 42, No. 135, pp. 9–18.

[18] Shi, H.H., and Takayama, K., 1995. Generation of high-speed liquid jets by high-speed impact of a projectile. JSME Int Series B J, Vol. 38, No. 2, pp. 181–190.

[19] Shi, H.H., Takayama, K., and Onodera, O. 1993. Experimental study of pulsed high-speed liquid jet. JSME Int Journal, Vol. 36 (4), Series B, pp. 620–627.

[20] Shi, H.H., and Takayama, K., 1999. Generation of hypersonic liquid fuel jets accompanying self-combustion. Shock Waves, Vol. 9, No. 5, pp. 327-332.

[21] Pianthong, K., 2002. Supersonic liquid diesel fuel jets; generation, shock wave; Characteristics, Auto-ignition Feasibilities. Ph.D. Thesis, Univ New South Wales, Sydney, Australia, pp. 1-259.

[22] Milton, B.E., and Pianthong, K., 2005. Pulsed, supersonic fuel jets - A review of their characteristics and potential for fuel injection. Int J Heat and Fluid Flow, Vol. 26, No. 4, pp. 656-671.

[23] Pianthong, K., Zakrzewski, S., Behnia, M., and Milton, B.E., 2002. Supersonic Liquid Jets: their generation and shock wave characteristics. Shock Waves, Vol. 11, No. 6, pp. 457-466.

[24] Pianthong, K., Milton, B.E., and Behnia, M., 2003. Generation and shock wave characteristics of unsteday pulsed supersonic liquid jets. Atomization and Sprays, Vol. 13, No. 5&6, pp. 475-498.

[25] Pianthong, K., Takayama, K., Milton, B.E., and Behnia, M., 2005. Multiple pulsed hypersonic liquid diesel fuel jets driven by projectile impact. Shock Waves, Vol. 14, No. 1&2, pp. 73-82.

[26] Pianthong, K., Zakrzewski, S., Milton, B.E., and Behnia, M., 2003. Characteristics of impact driven supersonic liquid jets. Exp Thermal and Fluid Sci, Vol. 27, No. 5, pp. 589-598.

[27] Takayama, K., 1983. Application of holographic interferometry to shock wave research. In: Fagan WF editor, Industrial applications of laser technology, SPIE 398, Bellingham: pp. 174–181.